Seismological Research Letters

The ShakeMap Atlas of historical earthquakes in Italy: configuration and validation

--Manuscript Draft--

Manuscript Number:	SRL-D-23-00138R2
Full Title:	The ShakeMap Atlas of historical earthquakes in Italy: configuration and validation
Article Type:	Focus Section - Seismic Hazard Modeling
Corresponding Author:	ILARIA OLIVETI, Ph.D Istituto Nazionale di Geofisica e Vulcanologia Roma, Italy ITALY
Corresponding Author Secondary Information:	
Corresponding Author's Institution:	Istituto Nazionale di Geofisica e Vulcanologia
Corresponding Author's Secondary Institution:	
First Author:	ILARIA OLIVETI, Ph.D
First Author Secondary Information:	
Order of Authors:	ILARIA OLIVETI, Ph.D
	Licia Faenza
	Andrea Antonucci
	Mario Locati
	Andrea Rovida
	Alberto Michelini
Order of Authors Secondary Information:	
Manuscript Region of Origin:	ITALY
Suggested Reviewers:	Susan Hough
	Trevor I. Allen
Opposed Reviewers:	

No changes have been made, except for the following corrections requested by the reviewer#3:

Line 35: "made since long" -> "made"
Line 55: "it has been .. Atlas" -> "version 4 of the Atlas has been released"
Line 180: "reveals to be" -> "is"
Line 302: "To this regard" -> "In this regard"
Line 383: "adjourned" -> "recalibrated"

The ShakeMap Atlas of historical earthquakes in Italy: configuration and validation

Ilaria Oliveti[1*], Licia Faenza[2], Andrea Antonucci[3], Mario Locati[3], Andrea Rovida[3], and Alberto Michelini[1]

[1]Istituto Nazionale di Geofisica e Vulcanologia, Sezione ONT, Rome, Italy.

[2]Istituto Nazionale di Geofisica e Vulcanologia, Sezione di Bologna, Bologna, Italy.

[3]Istituto Nazionale di Geofisica e Vulcanologia, Sezione di Milano, Milan, Italy.

[*]Corresponding author. Email: ilaria.oliveti@ingv.it

DECLARATION OF COMPETING INTERESTS

The authors acknowledge there are no conflicts of interest recorded.

ABSTRACT

Italy has a long tradition of studies on the seismic history of the country and the neighbouring areas. Several archives and databases dealing with historical earthquake data – primarily intensity data points – have been published and are constantly updated. Macroseismic fields of significant events are of foremost importance in assessing earthquake effects and for the

evaluation of seismic hazard. Here we adopt the USGS-ShakeMap software to calculate the maps of strong ground shaking (shakemaps) of 79 historical earthquakes with magnitude $\geq$ 6 that have occurred in Italy between 1117 and 1968 CE. We use the macroseismic data published in the Italian Macroseismic Database (DBMI15). The shakemaps have been determined using two different configurations. The first adopts the virtual intensity prediction equations approach (VIPE; i.e., a combination of ground motion models, GMMs, and ground motion intensity conversion equations, GMICEs; Bindi et al. (2011a); Oliveti et al. (2022b)). The second exploits the intensity prediction equations (IPE, Pasolini et al. (2008a); Lolli et al. (2019)). The VIPE configuration has been found to provide more accurate results after appraisal through a cross-validation analysis and has been applied for the generation of the ShakeMap Atlas. The resulting maps are published on the INGV ShakeMap (see Data and Resources; Oliveti et al., 2023), and on the ASMI (see Data and Resources; Rovida et al., 2017) platforms.

INTRODUCTION

Macroseismic intensity observations of past earthquakes can provide valuable constraints for reconstructing shaking distributions in the absence of instrumentally recorded data and are commonly used to estimate the location and magnitude of historical events (e.g., Teramo et al., 1996; Bakun and Wentworth, 1997; Gasperini et al., 2010; Beauval et al., 2010; Provost and Scotti, 2020, amongst others). Much effort has been made to aggregate the available data in comprehensive historical earthquake catalogs at both the national (e.g. Fäh et al., 2011; Manchuel et al., 2018; Rovida et al., 2020), and international scales (e.g., the European Preinstrumental Earthquake Catalogue EPICA; Rovida and Antonucci, 2021; Rovida et al., 2022a). These catalogs are fundamental for complementing and extending back in time instrumental earthquake catalogs for probabilistic seismic hazard assessment studies. In turn, it occurs that historical macroseismic intensities are the only long-term shaking data against which the outcomes of probabilistic seismic hazard studies can be tested, and sanity

checks be performed (Stirling and Petersen, 2006; Mucciarelli et al., 2008; Brooks et al., 2019).

However, depending on several historical, geographical and seismological factors, macroseismic intensity distributions of past earthquakes as inferred from historical documentation may present temporal and spatial gaps. Several methods exist in the literature to reconstruct and/or integrate the spatial distribution of the ground shaking of historical events, based on different approaches and assumptions (for a review, see Antonucci et al., 2021, and references therein). Among these, the established ShakeMap methodology (Wald et al., 1999) has been used for defining the ground shaking of historical earthquakes at both the global (e.g., Allen et al., 2008) and local scales (e.g., Schwarz et al., 2008; Faenza et al., 2013). In particular, Allen et al. (2008) developed the so-called ShakeMap Atlas, a compilation of peak ground motions and intensity maps for ∼14,100 recent and historical earthquakes worldwide. More recently, Version 4 of the Atlas has been released (see Data and Resources), including a vastly expanded compilation of shakemaps for consequential and widely felt earthquakes using the updated ShakeMap (Version 4) software. For historical earthquakes in the global ShakeMap Atlas, macroseismic intensity values often represent the only available observations, or provide valuable constraints, whereas strong-motion recordings are sparse (Allen et al., 2009b). The ShakeMap Atlas contributed to the development of fragility curves and loss model calibration (Luco and Karaca, 2007; García et al., 2012) and, to this end, provides a fundamental resource for the USGS Prompt Assessment of Global Earthquakes for Response (PAGER) system (Earle et al., 2009; Allen et al., 2009a) and the Earthquake Consequences Database (Crowley et al., 2013) within the Global Earthquake Model (GEM) initiative.

From the technical point of view, the ShakeMap Atlas includes direct empirical equations that estimate site intensity for a given earthquake magnitude and distance (IPEs, intensity prediction equations) to incorporate macroseismic intensity as a native ground motion parameter. According to the currently available peer-reviewed studies, IPEs strongly depend

on the selected data, and they differ in the approaches employed for the statistical analysis, such as the regression technique (e.g., Sørensen et al., 2009, amongst others) or the fully probabilistic method (e.g., Pasolini et al., 2008a). Due to the regional dependency of seismic characteristics, several studies developed regional or local intensity attenuation relations (e.g., Bakun, 2006; Bakun and Scotti, 2006; Stromeyer and Grünthal, 2009; Bindi et al., 2011b; Baumont et al., 2017; Oros et al., 2019, amongst others) for different regions of the world.

In the current study, we first produced shakemaps of strong (M≥6) Italian historical earthquakes using two different models implemented in the newly developed USGS-ShakeMap version 4 (Worden et al., 2020) by gathering intensity data from the Italian Macroseismic Database DBMI15 version 4.0 (see Data and Resources; Locati et al., 2022), and then selected the most appropriate configuration through the application of a ranking procedure consisting of statistical tests. In particular, we have considered for our configuration for the calculation of the intensity maps the Italian-derived IPE proposed by Pasolini et al. (2008a,b) recalibrated by Lolli et al. (2019), hereafter Pea08, and the default "virtual" IPE (Worden et al., 2017) available in ShakeMap, hereafter VIPE, as described in the ShakeMap Configuration section. The results obtained using the VIPE and Pea08 configurations have been appraised by analyzing the differences between the intensity predictions and the observed data using an iterative cross-validation procedure analysis (also known as leave-one-out analysis; Tomczak, 1998; Hofierka et al., 2007; Worden et al., 2010; Michelini et al., 2020). In addition, we have also investigated how the inclusion of finite faults affects the accuracy and the robustness of the ShakeMap prediction.

In summary, this work aims at presenting how we have developed the ShakeMap Atlas of historical earthquakes in Italy. To this goal, we have focused much attention to evaluate the accuracy of the selected configurations in order to provide a consistent and quantitative description of the distribution of shaking resulting from historical events in Italy.

DATA

Italy has a very long tradition of macroseismic investigation that produced a wealth of studies and data on the seismic history of the country and promoted the compilation of comprehensive historical macroseismic catalogues. The Italian Archive of Historical Earthquake Data ASMI (see Data and Resources, Rovida et al., 2017) collects more than 430 seismological studies, and grants access to a large number of intensity data from a variety of sources, such as macroseismic bulletins, online databases, and many scientific papers and reports. As a whole, it supplies data on more than 6500 Italian earthquakes in the period 461 B.C. to 2020 CE. The current release of the Italian Macroseismic Database DBMI (DBMI15, see Data and Resources, here considered in its version 4.0; Locati et al., 2022) is obtained by selecting, for each earthquake, data that are collected in ASMI according to their content, reliability, and quality, and to the number and spatial distribution of intensity data. DBMI15 version 4.0 contains 123981 Macroseismic Data Points (MDPs) related to 15343 populated places (from big towns to small villages) in Italy and 3229 earthquakes in the time-window 1000-2020 CE. In order to provide a homogeneous set of intensity data, DBMI15 applies the following standardization procedures to the original input data: i) a consistent gazetteer related to the Italian territory was adopted in order to unambiguously match a pair of geographical coordinates of each locality with the intensity value provided by the original study, ii) a standard based on Arabic numerals (e.g., 6, 6-7, 7) was used to express the macroseismic intensity, and iii) a set of descriptive codes (e.g., "HF" for Highly Felt, "SD" for Slightly Damage, "D" for Damage, "HD" for Heavy Damage) was adopted when the original data source does not assess a proper numerical intensity value, e.g., because the available information is not sufficient.

To generate the shakemaps, we extracted from DBMI15 the MDPs related to earthquakes with magnitudes equal to or greater than 6 that occurred before 1972, for which no instrumental ground motion recording exists according to the ITalian ACcelerometric Archive (ITACA; Russo et al., 2022). To this purpose, we improved the web service originally developed in the

framework of the EPOS Thematic Core Service for Seismology (Haslinger et al., 2022) for accessing macroseismic intensity data both in the European Archive of Historical Earthquake Data AHEAD (Locati et al., 2014; Rovida and Locati, 2015) and in the Italian Archive of Historical Earthquake Data ASMI (see Data and Resources). In particular, to the already supported XML, CSV and GeoJSON data encodings, we added an output format suitable for the ShakeMap software that wraps the required files into a zip package. The web-service recompiles the uncertain intensity values (e.g., 6-7 or 7-8) as half degrees (e.g., 6.5 or 7.5), according to the standard adopted in DBMI15 (see Rovida et al., 2020).

The dataset used for testing the ShakeMap configurations and generating the shaking maps includes 79 earthquakes that occurred between January 1117 and January 1968 with $6 \leq M \leq 7.3$ according to the Italian Parametric Earthquake Catalogue CPTI15 (Rovida et al., 2020, 2022b, Figure 1). The main characteristics of the selected events according to CPTI15 are reported in Table 1, in terms of origin time, epicentral location, magnitude, number of MDPs, name of the epicentral area and reference macroseismic study.

The intensities provided by DBMI15 for the considered earthquakes are assessed in the Mercalli-Cancani-Sieberg scale (MCS; Sieberg, 1923), and MDPs with descriptive intensity codes were not included in the dataset because they represents data for which the available information is not considered sufficient for assessing any intensity value. As a result, our dataset consists of 12632 MDPs in total, and the number of available data per earthquake is extremely variable (Table 1), with a minimum of 2 MDPs for the July 17, 1361 earthquake (M 6.3) and a maximum of 1366 MDPs for the February 23, 1887 earthquake (M 6.3). As shown in Figure 2, the number of MDPs of the entire dataset (and of the single events) increases through time. This increase results from the low intensity values that start to be represented significantly only after ∼1850 (see earthquake number 63 and subsequent ones in Figure 2). In contrast, the number of the highest intensities in the dataset is rather uniform through time (Figure 2). This is in agreement with the historical analysis of the time series of significant earthquake effects of Stucchi et al. (2004) who concluded that the

completeness for intensities higher than degree 8 might start as far back as the 12th century, depending on the area. In addition, it is noteworthy to point out that our dataset consists of strong earthquakes whose intensities are homogeneously assessed with a-posteriori analyses of earthquake records provided by archival documentation (see Guidoboni and Stucchi, 1993; Guidoboni and Ferrari, 2000; Camassi, 2004). This implies that the macroseismic assessment of historical earthquakes is conducted by professional historians according to the methods of historiographic research, i.e., taking into account the specific temporal, cultural, social, and geo-political contexts in which the records were produced (see Guidoboni and Ebel, 2009).

In Figure 3 we make an attempt to verify whether any prominent bias affects the dataset used to determine our ShakeMap Atlas. All the panels graph the MDPs as distance from the earthquake versus intensity. In the panels on the left hand side (lhs) (Figure 3a, c, e), the MDPs are shown according to three time slots (1000-1399, 1400-1799, and 1800-2020). On the right hand side (rhs) (Figure 3b, d, f), the MDPs are grouped according to three magnitude ranges (6.0-6.5, 6.5-7.0, and 7-7.5). The panels to left and right appear to confirm that no significant bias (i.e., larger number of higher intensities) exists for the older events. The same panels evidence also that the intensities lower than or equal to 6 are poorly represented in the dataset, due to a possible incompleteness of the far field data of strong historical earthquakes (Antonucci et al., 2023). The panels in which the MDPs are grouped by magnitude (rhs),show that as the magnitude increases there is the expected shift towards larger distances of the higher intensities. The temporal color scale reflects the MDPs distribution of the lhs panels. In general, this figure shows that about a quarter (24.02%) of MDPs has distances from the earthquake larger than 100 km. As far as short distances are concerned, MDPs with intensity value greater than 7 are prevalent.

SHAKEMAP CONFIGURATION

ShakeMap is an interpolation algorithm that makes use of recorded data and seismological and geotechnical knowledge to produce maps of ground motion at local and regional scales.

Thus, in addition to the observations, the prediction equations expressed in terms of peak ground motion parameters, the so-called ground-motion models (GMMs), and the intensity prediction equations (IPEs) are indispensable in ShakeMap to supplement the generally sparse and incomplete available data. In addition, Vs30, defined as the average seismic shear-wave velocity from the surface to a depth of 30 meters, is important for estimating local site amplifications of the ground motion. Specifically, ShakeMap accounts for the local site amplifications using an equally spaced grid of Vs30 values. When site classes are the only available information (e.g., Eurocode 8 [EC8] soil categories), they need to be converted into the corresponding Vs30 values (see Michelini et al., 2020, for Italy). A comprehensive explanation of how site effects are integrated into ShakeMap can be found in the detailed description provided by Worden et al. (2017). Moreover, GMICEs (ground motion to intensity conversion equations) are adopted wherever macroseismic intensities have to be transformed into ground motion parameters as, for example, when macroseismic data are used as input for generating ground motion maps and vice-versa (i.e., when estimating the macroseismic intensity field from recorded instrumental peak ground motion parameters). Therefore, the selection of the proper set of equations plays a key role in accurately estimating the shaking.

The application of an updated method to the interpolation process (Worden et al., 2018; Engler et al., 2022) to generate the shakemaps allows for more rigorous estimates of ground shaking and proper accounting of associated uncertainties when conditioned on geographically distributed strong-motion station data or macroseismic intensity observations. According to this method, the interpolation in ShakeMap is performed by treating the ground motions (or the intensities) as a conditional multivariate normal distribution (MVN). This approach, in combination with a GMM and cross-correlation functions among the available data, provides a flexible framework for estimating the ground shaking at arbitrary locations. For quantifying the uncertainty in these estimates, this technique also preserves the separation of the conditioned residuals into between-event (perfectly correlated) and within-event

(spatially correlated) spatial processes (Engler et al., 2022).

In this work, to the purpose of identifying the most accurate ground shaking field of past historical earthquakes, we have computed the shakemap set (Worden et al., 2020), i.e., maps of macroseismic intensity, and five intensity measures — peak ground acceleration (PGA), peak ground velocity (PGV), and spectral acceleration (SA) ordinates at 0.3, 1.0, and 3.0 s, respectively, using two different configurations. For what concerns the generation of the "macroseismic intensity" maps, the first configuration adopts the default VIPE, whereas the second one implements the IPE proposed by Pasolini et al. (2008a,b), updated by Lolli et al. (2019). We remark, however, that for both configurations we have generated the maps of PGA, PGV, and SA adopting (1) the GMMs selected by Michelini et al. (2020) accounting for the subdivision of Italy in different tectonic regimes and (2) the GMICEs of Oliveti et al. (2022b) calibrated on the dataset by Oliveti et al. (2022a) for the conversion between ground motion and macroseismic intensity.

With regard to the first point, Michelini et al. (2020) identified the most suitable GMMs to be utilized in each region based on the GMM zonation proposed by Visini et al. (2022) for the Italian seismic hazard model MPS19 (Meletti et al., 2021). In particular, Michelini et al. (2020) validated this configuration within ShakeMap evidencing a substantial improvement in the accuracy of ground-motion estimates for Italy. Since all earthquakes in our validation dataset fall within the shallow active crustal region (SACR), both the VIPE and Pea08 configurations use the Bindi et al. (2011a) GMM that is used for the SACR tectonic regime and shallow depth earthquakes.

As for the second point, the reversible GMICEs proposed by Oliveti et al. (2022b) correlate the maximum horizontal component of recorded PGA, PGV, and SA at T = 0.3, 1.0 and 3.0 s to macroseismic intensity values for Italy. Specifically, Oliveti et al. (2022b) adopted the common current approach involving a regression for the intensity as a function of the PGM parameters and viceversa, resulting in magnitude-distance-independent conversions, showing no significant trend of the residuals for both magnitude and distance. Very recently,

two new different methodologies have been introduced by Gallahue and Abrahamson (2023) to develop GMICEs. The authors state that the GMICEs developed using their approaches lead to more accurate estimates of the intensities than currently adopted methodologies. Here we note, however, that the comparison made by Oliveti et al. (2022b) with similar regressions previously published for Italy (e.g., Faenza and Michelini, 2010, 2011; Zanini et al., 2019; Masi et al., 2020; Cataldi et al., 2021, amongst others) demonstrates that the proposed relationships provide significantly improved fits to the data regardless. Moreover, to further validate their effectiveness, these relations were tested within the ShakeMap system of the Italian configuration, showing very accurate estimates of shaking and minimal bias.

In the present study, VIPE is a combination of selected GMM and associated GMICEs, which, combined together, offer the same interface and behavior of an IPE. This makes VIPE inherently valid for a broader range of regional and tectonic environments but it also entails increased uncertainty in the estimated intensity values compared to the currently available IPEs. Generally, VIPE is used in ShakeMap when the operator does not specify an IPE. The related module predicts the ground motion through the GMM and converts it to intensity using the GMICEs. In detail, it first attempts to use PGV for the calculation of the intensities, and then tries PGA, and then SA(1.0).

By contrast, Pea08 is a specific Italian macroseismic intensity attenuation model calibrated as a function of moment magnitude and epicentral distance (Pasolini et al., 2008a). A recalibration of Pea08 was done by Lolli et al. (2019) using the updated intensity data points from DBMI15 (Locati et al., 2022) and earthquake parameters provided by CPTI15 (Rovida et al., 2022b). As a result, the macroseismic intensity attenuation model proposed by Lolli et al. (2019) has the same functional form of the equation of Pasolini et al. (2008a) but different values of parameters.

Since ShakeMap requires as input the hypocentral depth, and CPTI15 does not provide this information when the instrumental epicentre is not available, we arbitrarily assigned a value of 10 km to all the analyzed historical earthquakes (see Table 1). However, our

results are not affected by this choice because the ground motion model adopted is based on epicentral distance and the IPEs are not depth-dependent relationships either.

COMPARISON BETWEEN IPE AND VIPE IMPLEMENTATION

In this section, we present the results of the tests on the two selected configurations (i.e. using VIPE and Pea08, respectively) to show their accuracy in predicting the intensity value at the macroseismic data points. To this end, we adopted an iterative cross-validation procedure that performs the following steps for each observed intensity. Select a target earthquake and, iteratively, for each MDP:

- remove the MDP from the dataset;
- use the ShakeMap procedure to predict the intensity at the removed MDP (i.e., while keeping all the others);
- compute the difference between the observed and predicted intensity value at the removed MDP.

This procedure has been repeated for all the earthquakes selected. For the validation analysis, we computed the shakemaps using Pea08 and VIPE separately as input. For both configurations, we used the same values for the source parameters (e.g., hypocenter and magnitude), and the GMM, site effects and GMICEs mentioned above.

It is important to note that the intensity predictions were not derived for the total number of observed data extracted from DBMI15, i.e. 12632. First, we removed from further processing all the data points located outside the ShakeMap regular grid (i.e., a finely-sampled grid - nominally 1km spacing - of latitude and longitude pairs, whose dimensions depend on the earthquake magnitude). As a result, only 12299 MDPs were used initially for the cross-validation analysis. Then, ShakeMap's automatic removal of outliers (i.e., observations that exceed two standard deviations above or below the prediction) reduced the number of data points ensuring the calculation of robust maps of ground shaking. In

our case, this quality assurance protocol found 115 and 377 outliers using VIPE and Pea08, respectively, showing a better performance in predicting intensity of the former over the latter. Finally, we also removed MDPs not common to both datasets obtained using the two models. This step is needed to ensure that the comparison occurs only among the same observed points. In summary, the entire data processing resulted in a final validation dataset with a total of 11885 MDPs.

The results of the cross-validation analysis for all the earthquakes are presented as differences between observed and predicted intensity values (i.e., residuals) through the violin plot representations in Figure 4.

Figure 4a shows that the median value for both models is close to zero, whereas the standard deviation calculated using VIPE is smaller than that obtained adopting Pea08. This indicates that both configurations do not suffer from significant systematic bias, but VIPE shows a smaller scatter in the residuals than Pea08.

When the data are grouped according to the EC8 site classes (Fig. 4b-d), we observe overall the same behavior described for the entire dataset (Fig. 4a). If we focus our attention to the disaggregated results in Figure 4c-d, we note that median values close to zero are found for the EC8 B–C soil site classes, which extend over a significant part of the Italian territory (CEN, 2004) and, consequently, over the great part of the selected localities. Conversely, in Figure 4b positive median values for the EC8 site class A indicate a slight underprediction of the level of intensity predicted by VIPE. This latter trend is likely due to VIPE using the configured GMM for predicting ground motion. In this regard, Michelini et al. (2020) explained it as due to inappropriate attribution of the EC8 soil site class A to stations effectively sited on softer and more amplifying soils. In contrast, Pea08 does not include site-amplification factors for implementing site effects, and the residuals do not suffer from the same underprediction.

Table 2 shows the mean, median, standard deviation, first and third quartiles of the distribution of the residuals for the entire dataset and for the EC8 A-C classes disaggregated

subsets. The standard deviations of the residuals vary between 0.15 and 0.22 for VIPE, and between 0.23 and 0.24 for Pea08. The first and third quartiles range between -0.11 and 0.06 for VIPE, except for Q3 which equals 0.23 for EC8 class A, whereas the same parameters for Pea08 feature larger values, i.e. between -0.13 and 0.14.

While VIPE offers better predictions at the MDPs, it comes at the cost of higher uncertainty in these predicted intensity values than Pea08. In the case of Pea08, the uncertainty at the observation site is assumed to be zero, whereas, at the predicted points, it is assumed to have a non-zero uncertainty due to the spatially averaged nature of intensity assignments. More specifically, the uncertainty for estimates from Pea08 is the stated uncertainty given in Lolli et al. (2019) conditioned on geographically distributed macroseismic intensity observations, as described in the ShakeMap Configuration section. By contrast, for VIPE, an additional uncertainty associated with the conversion itself (i.e., the uncertainty of the GMICEs) results in the predictions. This is due to the three-step procedure adopted in ShakeMap when using VIPE, that first converts intensities to peak ground motions (PGMs) using the GMICEs, then uses the GMM to supplement sparse data in its interpolation and estimation of ground motions, and finally converts the PGMs back to intensities using the GMICEs. In particular, the standard deviation of the predicted intensity calculated using VIPE is given by the rules of error propagation (Ku et al., 1966). In practice, the uncertainty in the predicted intensity values is computed by combining the uncertainty of the GMM with the uncertainty of the GMICEs. This is confirmed by the results illustrated in Figure 5. The histograms of Figure 5 show the distribution of the standard deviation of the predicted intensity values, for both VIPE and Pea08, as calculated by ShakeMap.

Additional tests were carried out to explore the behavior of the calculated residuals with distance from the earthquake (Fig. 6a) and intensity value (Fig. 6b), respectively. The residuals obtained using either VIPE or Pea08 are very close to zero when considering all the distances and the intensity classes, except for intensities lower than 4-5. This leads us to state that ShakeMap slightly overestimates the intensity values when compared to the

observed data. A possible explanation for this behavior comes from the magnitude range of the earthquakes in our dataset ($M \geq 6.0$) that feature few low value intensities (less than 4-5), at long earthquake distances as shown in Figure 3. Other factors, however, more related to the calibration of Pea08 and the adopted GMM (Bindi et al., 2011a) can account for the low shaking and they cannot be excluded. Furthermore, we observed that, in all cases shown in Figure 6a-b, the residuals calculated using VIPE perform better than those obtained adopting Pea08, which show many outliers and much scattered data.

In order to verify if the accuracy of the intensity predictions improves when the finiteness of the source dimensions are considered, the leave-one-out cross-validation analysis was applied to a subset of the original dataset using VIPE. We selected the faults and the focal mechanism parameters from the Database of Individual Seismogenic Sources (DISS, see Data and Resources; DISS Working Group, 2021) matching each selected earthquake with a fault whenever possible. As a result, we found that for only 16 earthquakes we could identify the appropriate fault (Table 3). We then used the leave-one-out cross-validation technique as above to test the goodness of the selected configuration considering a total of 4799 MDPs. The violin plot diagrams of Figure 7 show the distribution of the differences between the configuration with and without the fault geometry at all the intensity points. Figure 7 shows no significant improvement in the prediction performance when including the finite faults. The same comparison cannot be made for the configuration that adopts Pea08 because this IPE depends only on epicentral distance. In fact, one feature of ShakeMap is that it considers the actual rupture plane (or its surface projection) rather than the epicenter, when the fault is included in the processing.

Overall, our results evidence the goodness of VIPE in predicting the intensity data within the ShakeMap algorithm. Since VIPE is computed by combining the GMM by Bindi et al. (2011a) and the GMICEs by Oliveti et al. (2022b), our tests are crucial to cross-verify the consistency of these relationships. This relevant observation confirms the ShakeMap accuracy in estimating the shaking when adopting proper GMMs and GMICEs.

The intensity maps shown in Figure 8 have been obtained with the investigated configurations (i.e. using VIPE and Pea08) and were drawn as examples from the entire ShakeMap Atlas of historical earthquakes in Italy (see Data and Resources). These include the 5 December 1456 M 7.2, the 27 March 1638 M 7.1, and the 13 January 1915 M 7.1 earthquakes. They have been selected since they all resulted in significant fatalities and damage. More specifically, the December 1456 M 7.2 earthquake resulted in over 10,000 deaths (Meletti et al., 1988), whereas the other two events caused the deaths of nearly 30,000 people (Guidoboni et al., 2007; Molin et al., 1999, respectively). With regard to the comparison between the maps obtained using the two different configurations, we note that the selected earthquakes seem well suited to this end since they all have a large number of MDPs. In general, the VIPE configuration appears to generate slightly larger intensity values when compared to Pea08 at large earthquake distances.

CONCLUSIONS

In this work, we appraised two different USGS-ShakeMap configurations to compute the ShakeMap Atlas of large historical earthquakes in Italy using the available macroseismic data. To this end, we produced a shakemap set, in terms of macroseismic intensity, PGA, PGV, and SA at 0.3s, 1.0s, and 0.3s, for 79 earthquakes with magnitude ≥ 6 between 1117 and 1968 CE.

We identified the most appropriate configuration between VIPE (i.e., the combination of the selected GMM and GMICEs) and the (direct) IPE proposed by Pasolini et al. (2008a) and recalibrated by Lolli et al. (2019), through the adoption of an iterative cross-validation procedure within ShakeMap. To convert from macroseismic intensities to peak ground motion (and viceversa), we adopted the configuration of ShakeMap described by Michelini et al. (2020) and the GMICEs proposed by Oliveti et al. (2022b). To assess the accuracy of the results obtained using the two configurations, we used the leave-one-out cross-validation analysis applied to the macroseismic intensity points within ShakeMap. Our analysis of the

residuals (i.e., the differences between the observed and predicted intensity data) obtained with VIPE and Pea08 shows that, overall, the former predicts more accurately the intensity values for all the MDPs irrespective of distance and EC8 soil class type. The only exception is represented by the EC8 A class (hard rock) which shows some slight underestimation of the predicted intensities. The leave-one-out cross-validation analysis was also applied to estimate the intensity prediction capabilities when the finite fault is available to find that it does not improve significantly the accuracy of the intensity estimates.

In conclusion, the proposed configuration using VIPE appears to provide accurate macroseismic intensity estimates for historical earthquakes in Italy. The resulting shakemaps are available on the INGV ShakeMap (see Data and Resources; Oliveti et al., 2023), and on the ASMI platforms (see Data and Resources; Rovida et al., 2017).

DATA AND RESOURCES

The earthquakes have been selected from the Parametric Catalogue of Italian Earthquakes CPTI15 Version 4.0 (`https://doi.org/10.13127/CPTI/CPTI15.4`) and a tabular list is provided in Table 1. The intensity observations are all accessible on the Version 4.0 of the Italian Macroseismic Database DBMI15 through the ShakeMap webservices (`https://emidius.mi.ingv.it/services/macroseismic/`). The U.S. Geological Survey (USGS)-ShakeMap open-source software is available on the GitHub development platform (`https://github.com/usgs/shakemap`). The shakemaps presented in this paper (`https://doi.org/10.13127/shakemaps/historical)` are available at `http://shakemap.ingv.it/shake4/`, through the web portal of the Italian Archive of Historical Earthquake Data ASMI (`https://doi.org/10.13127/asmi`). The USGS ShakeMap Atlas is available at `https://earthquake.usgs.gov/data/shakemap/atlas/`. Version 3.3.0 of the Database of Individual Seismogenic Sources (DISS) is available at `https://doi.org/10.13127/diss3.3.0`. OpenQuake library of modern ground-shaking intensity models is available at `https://https://docs.openquake.org/oq-engine/3.13/_modules/openquake/hazardlib/gsim/`. Some analy-

ses and plots are made using ObsPy (Beyreuther et al., 2010; Megies et al., 2011; Krischer et al., 2015) and the Python pandas software (`https://pandas.pydata.org`).

ACKNOWLEDGMENTS

This research was supported by the "Istituto Nazionale di Geofisica e Vulcanologia" and the "Dipartimento Protezione Civile" under 2019-2021 B2-WP1, Task 5 "ShakeMap adjournment project" and Task 1 "Integration of historical seismology databases". This study has benefited from funding provided by the Italian Presidenza del Consiglio dei Ministri – Dipartimento della Protezione Civile (DPC). This paper does not necessarily represent DPC official opinion and policies. The authors thank S. Hough and an anonymous reviewer who provided constructive and helpful comments on an earlier version of this paper.

References

Allen, T. I., Marano, K. D., Earle, P. S. and Wald, D. J. (2009a) Pager-cat: A composite earthquake catalog for calibrating global fatality models. *Seismological Research Letters*, **80**, 57–62.

Allen, T. I., Wald, D. J., Earle, P. S., Marano, K. D., Hotovec, A. J., Lin, K. and Hearne, M. G. (2009b) An atlas of shakemaps and population exposure catalog for earthquake loss modeling. *Bulletin of Earthquake Engineering*, **7**, 701–718.

Allen, T. I., Wald, D. J., Hotovec, A. J., Lin, K., Earle, P. S. and Marano, K. D. (2008) *An Atlas of ShakeMaps for selected global earthquakes*. US Department of the Interior, US Geological Survey.

Antonucci, A., Rovida, A., D'Amico, V. and Albarello, D. (2021) Integrating macroseismic intensity distributions with a probabilistic approach: an application in italy. *Natural Hazards and Earth System Sciences*, **21**, 2299–2311.

— (2023) Looking for undocumented earthquake effects: a probabilistic analysis of italian macroseismic data. *Natural Hazards and Earth System Sciences*, **23**, 1805–1816.

Bakun, W. (2006) Estimating locations and magnitudes of earthquakes in southern california from modified mercalli intensities. *Bulletin of the Seismological Society of America*, **96**, 1278–1295.

Bakun, W. H. and Scotti, O. (2006) Regional intensity attenuation models for france and the estimation of magnitude and location of historical earthquakes. *Geophysical Journal International*, **164**, 596–610.

Bakun, W. u. and Wentworth, C. (1997) Estimating earthquake location and magnitude from seismic intensity data. *Bulletin of the Seismological Society of America*, **87**, 1502–1521.

449 Barbano, M. S., Gentile, G. F. and Riggio, A. M. (1986) Il terremoto dell'alpago-cansiglio
450 del 18.10.1936: metodologia e problematiche legate allo studio di eventi recenti. In *Atti*
451 *del 5° Convegno Annuale del GNGTS*, 47–60.

452 Barbano, M. S., Riggio, A. M., Catalan, T., Sclippa, P. and Toffoli, D. (1990) *Revisione*
453 *di alcuni terremoti dell'Italia nord-orientale nella prima metà del XX secolo*. Gruppo
454 Nazionale per la Difesa dai Terremoti, Udine.

455 Baumont, D., Manchuel, K., Traversa, P., Durouchoux, C., Nayman, E. and Ameri, G.
456 (2017) Empirical intensity attenuation models calibrated in mw for metropolitan france.
457 *Bull Earthq Eng*.

458 Beauval, C., Yepes, H., Bakun, W. H., Egred, J., Alvarado, A. and Singaucho, J.-C. (2010)
459 Locations and magnitudes of historical earthquakes in the sierra of ecuador (1587–1996).
460 *Geophysical Journal International*, **181**, 1613–1633.

461 Beyreuther, M., Barsch, R., Krischer, L., Megies, T., Behr, Y. and Wassermann, J. (2010)
462 Obspy: A python toolbox for seismology. *Seismological Research Letters*, **81**, 530–533.

463 Bindi, D., Pacor, F., Luzi, L., Puglia, R., Massa, M., Ameri, G. and Paolucci, R. (2011a)
464 Ground motion prediction equations derived from the italian strong motion database.
465 *Bulletin of Earthquake Engineering*, **9**, 1899–1920.

466 Bindi, D., Parolai, S., Oth, A., Abdrakhmatov, K., Muraliev, A. and Zschau, J. (2011b)
467 Intensity prediction equations for central asia. *Geophysical Journal International*, **187**,
468 327–337.

469 Brooks, E. M., Neely, J., Stein, S., Spencer, B. D. and Salditch, L. (2019) Assessments of
470 the performance of the 2017 one-year seismic-hazard forecast for the central and eastern
471 united states via simulated earthquake shaking data. *Seismological Research Letters*, **90**,
472 1155–1167.

Camassi, R. (2004) Catalogues of historical earthquakes in italy. *Annals of Geophysics*, **47**, 645–657. URL: `https://doi.org/10.4401/ag-3329`.

Camassi, R., Bernardini, F., Castelli, V. and Meletti, C. (2008) A 17th century destructive seismic crisis in the gargano area: Its implications on the understanding of local seismicity. *Journal of Earthquake Engineering*, **12**, 1223–1245.

Camassi, R., Caracciolo, C., Castelli, V. and Slejko, D. (2011) The 1511 eastern alps earthquakes: a critical update and comparison of existing macroseismic datasets. *Journal of Earthquake Engineering*, **15**, 191–213.

Camassi, R., Caracciolo, C. H., Castelli, V., Ercolani, E., Bernardini, F., Albini, P. and Rovida, A. (2012) *Contributo INGV al WP2 del progetto HAREIA - Historical and Recent Earthquakes in Italy and Austria: Studio della sismicità storica del Friuli Venezia-Giulia, Veneto e Alto Adige*. Istituto Nazionale di Geofisica e Vulcanologia, Roma.

Caracciolo, C. H., Camassi, R. and Castelli, V. (2015) *Il terremoto del 25 gennaio 1348 (Alpi orientali)*. Istituto Nazionale di Geofisica e Vulcanologia, Roma.

Castelli, V. (2003) *Revisione delle conoscenze sui terremoti del 1558 (Valdambra), 1561 (Campania-Basilicata), 1639 (Amatriciano) e 1747 (Nocera Umbra-Gualdo Tadino)*. Istituto Nazionale di Geofisica e Vulcanologia, Milano.

Castelli, V., Galli, P., Camassi, R. and Caracciolo, C. (2008) The 1561 earthquake(s) in southern italy: New insights into a complex seismic sequence. *Journal of Earthquake Engineering*, **12**, 1054–1077.

Castelli, V., Monachesi, G., Moroni, A. and Stucchi, M. (1996) *I terremoti toscani dall'anno 1000 al 1880: schede sintetiche*. Gruppo Nazionale per la Difesa dai Terremoti, Macerata-Milano.

Cataldi, L., Tiberi, L. and Costa, G. (2021) Estimation of mcs intensity for italy from high quality accelerometric data, using gmices and gaussian naive bayes classifiers. *Bulletin of Earthquake Engineering*, **19**, 2325–2342.

CEN (2004) Eurocode 8: Design of structures for earthquake resistance-part 1: general rules, seismic actions and rules for buildings. *Brussels: European Committee for Standardization,Brussels, Belgium, Directive 98/34/EC, Directive 2004/18/EC*.

Crowley, H., Pinho, R., Pagani, M. and Keller, N. (2013) Assessing global earthquake risks: the global earthquake model (gem) initiative. In *Handbook of seismic risk analysis and management of civil infrastructure systems*, 815–838. Elsevier.

DISS Working Group (2021) Database of individual seismogenic sources (DISS), version 3.3.0: A compilation of potential sources for earthquakes larger than m 5.5 in italy and surrounding areas [Data set]. URL: `https://doi.org/10.13127/diss3.3.0`.

Earle, P. S., Wald, D. J., Jaiswal, K. S., Allen, T. I., Hearne, M. G., Marano, K. D., Hotovec, A. J. and Fee, J. M. (2009) Prompt assessment of global earthquakes for response (pager): A system for rapidly determining the impact of earthquakes worldwide. *US Geological Survey Open-File Report*, **1131**, 15.

Engler, D. T., Worden, C. B. and Thompson, Eric M. ans Jaiswal, K. S. (2022) Partitioning ground motion uncertainty when conditioned on station data. *Bulletin of the Seismological Society of America*, **112(2)**, 1060–1079.

Faenza, L. and Michelini, A. (2010) Regression analysis of MCS intensity and ground motion parameters in Italy and its application in ShakeMap. *Geophysical Journal International*, **180**, 1138–1152.

— (2011) Regression analysis of MCS intensity and ground motion spectral accelerations (SAs) in Italy. *Geophysical Journal International*, **186**, 1415–1430.

Faenza, L., Pierdominici, S., Camassi, R., Michelini, A., Ercolani, E. and Lauciani, V. (2013) The shakemap atlas for the city of naples, italy. *Seismological Research Letters*, **84**, 963–972.

Fäh, D., Giardini, D., Kästli, P., Deichmann, N., Gisler, M., Schwarz-Zanetti, G., Álvarez Rubio, S., Sellami, S., Edwards, B., Allmann, B., Bethmann, F., Wössner, J., Gassner-Stamm, G., Fritsche, S. and Eberhard, D. (2011) ECOS-09 earthquake catalogue of switzerland, release 2011. report and database. *Tech. Rep. Report SED/RISK/R/001/20110417*, Swiss Seismological Service ETH Zurich.

Gallahue, M. and Abrahamson, N. (2023) New methodology for unbiased ground-motion intensity conversion equations. *Bulletin of the Seismological Society of America*, **113**, 1133–1151.

Galli, P. and Molin, D. (2007) *Il terremoto del 1905 della Calabria Meridionale. Studio Analitico degli effetti ed ipotesi sismogenetiche*. Il Mio Libro.

Galli, P., Molin, D., Galadini, F. and Giaccio, B. (2002) Aspetti sismotettonici del terremoto irpino del 1930. In *n: Castenetto S. and Sebastiano M. (eds.), Il "terremoto del Vulture" 23 luglio 1930, VIII dell'Era fascista* (eds. S. Castenetto and M. Sebastiano), 217–262. Servizio Sismico Nazionale, Roma.

Galli, P. and Naso, G. (2008) The taranta effect of the 1743 earthquake in salento (apulia, southern italy). *Bollettino di Geofisica Teorica e Applicata*, **49**, 177–204.

Galli, P. and Naso, J. A. (2009) Unmasking the 1349 earthquake source (southern italy): paleoseismological and archaeoseismological indications from the aquae iuliae fault. *Journal of Structural Geology*, **31**, 128–149.

García, D., Mah, R., Johnson, K., Hearne, M., Marano, K., Lin, K., Wald, D., Worden, C. and So, E. (2012) Shakemap atlas 2.0: An improved suite of recent historical earthquake

shakemaps for global hazard analyses and loss model calibration. In *World conference on earthquake engineering*.

Gasperini, P., Vannucci, G., Tripone, D. and Boschi, E. (2010) The location and sizing of historical earthquakes using the attenuation of macroseismic intensity with distance. *Bulletin of the Seismological Society of America*, **100**, 2035–2066.

Gizzi, F. T. (2012) *Il 'Terremoto Bianco' del 21 Agosto 1962. Aspetti macrosismici, geologici, risposta istituzionale*. Zaccara Editore.

Guidoboni, E. and Ebel, J. E. (2009) *Earthquakes and Tsunamis in the Past: A Guide to Techniques in Historical Seismology*. Cambridge University Press.

Guidoboni, E. and Ferrari, G. (2000) Historical variables of seismic effects: economic levels, demographic scales and building techniques. *Annals of Geophysics*, **43**, 687–706. URL: `https://doi.org/10.4401/ag-3663`.

Guidoboni, E., Ferrari, G., Mariotti, D., Comastri, A., Tarabusi, G. and Valensise, G. (2007) CFTI4Med, Catalogue of Strong Earthquakes in Italy (461 B.C.-1997) and Mediterranean Area (760 B.C.-1500) [Data set]. *Istituto Nazionale di Geofisica e Vulcanologia (INGV)*. URL: `http://storing.ingv.it/cfti4med/`.

Guidoboni, E. and Stucchi, M. (1993) The contribution of historical records of earthquakes to the evaluation of seismic hazard. *Annals of Geophysics*, **36**, 201–215. URL: `https://doi.org/10.4401/ag-4264`.

Haslinger, F., Basili, R., Bossu, R., Cauzzi, C., Cotton, F., Crowley, H., Custodio, S., Danciu, L., Locati, M., Michelini, A., Molinari, I., Ottemöller, L. and Parolai, S. (2022) Coordinated and interoperable seismological data and product services in europe: the EPOS thematic core service for seismology. *Annals of Geophysics*, **65**, DM213.

Hofierka, J., Cebecauer, T. and Šúri, M. (2007) Optimisation of interpolation parameters using cross-validation. In *Digital Terrain Modelling*, 67–82. Springer.

Krischer, L., Megies, T., Barsch, R., Beyreuther, M., Lecocq, T., Caudron, C. and Wassermann, J. (2015) Obspy: A bridge for seismology into the scientific python ecosystem. *Computational Science & Discovery*, **8**, 014003.

Ku, H. H. et al. (1966) Notes on the use of propagation of error formulas. *Journal of Research of the National Bureau of Standards*, **70**.

Locati, M., Camassi, R., Rovida, A., Ercolani, E., Bernardini, F., Castelli, V., Caracciolo, C. H., Tertulliani, A., Rossi, A., Azzaro, R. et al. (2022) Database macrosismico italiano DBMI15, versione 4.0.

Locati, M., Rovida, A., Albini, P. and Stucchi, M. (2014) The ahead portal: a gateway to european historical earthquake data. *Seismological Research Letters*, **85**, 727–734.

Lolli, B., Pasolini, C., Gasperini, P. and Vannucci, G. (2019) Prodotto 4.8: Ricalibrazione dell'equazione di previsione di pasolini et al. (2008). In *Meletti, C. e Marzocchi W. (a cura di), II modello di pericolosità sismica MPS19. Rapporto finale*, 99. Centro Pericolosità Sismica, Istituto Nazionale di Geofisica e Vulcanologia, Roma.

Luco, N. and Karaca, E. (2007) Extending the usgs national seismic hazard maps and shakemaps to probabilistic building damage and risk maps. In *Proceedings of the 10th Int'l Conf. on Applications of Statistics and Probability in Civil Engineering*.

Manchuel, K., Traversa, P., Baumont, D., Cara, M., Nayman, E. and Durouchoux, C. (2018) The french seismic CATalogue (FCAT-17). *Bulletin of Earthquake Engineering*, **16**, 2227–2251.

Masi, A., Chiauzzi, L., Nicodemo, G. and Manfredi, V. (2020) Correlations between macro-

seismic intensity estimations and ground motion measures of seismic events. *Bulletin of Earthquake Engineering*, **18**, 1899–1932.

Megies, T., Beyreuther, M., Barsch, R., Krischer, L. and Wassermann, J. (2011) Obspy–what can it do for data centers and observatories? *Annals of Geophysics*, **54**, 47–58.

Meletti, C., Marzocchi, W., D'amico, V., Lanzano, G., Luzi, L., Martinelli, F., Pace, B., Rovida, A., Taroni, M., Visini, F. et al. (2021) The new italian seismic hazard model (mps19). *Annals of Geophysics*, **64**.

Meletti, C., Patacca, E., Scandone, P. and Figliuolo, B. (1988) Il terremoto del 1456 e la sua interpretazione nel quadro sismotettonico dell'appennino meridionale. In *Figliuolo B. (ed), Il terremoto del 1456*, 167. Osservatorio Vesuviano, Napoli.

Michelini, A., Faenza, L., Lanzano, G., Lauciani, V., Jozinović, D., Puglia, R. and Luzi, L. (2020) The new shakemap in italy: Progress and advances in the last 10 yr. *Seismological Research Letters*, **91**, 317–333.

Molin, D., Galadini, F., Galli, P., Mucci, L. and A., R. (1999) Il terremoto del 1456 e la sua interpretazione nel quadro sismotettonico dell'appennino meridionale. In *Castenetto S., Galadini F. (eds.), 13 gennaio 1915. Il terremoto nella Marsica*, 30. Servizio Sismico Nazionale, Roma.

Monachesi, G. (1987) *Revisione della sismicità di riferimento per i comuni di Cerreto d'Esi (AN), Esanatoglia (MC), Serra San Quirico (AN).* Osservatorio Geofisico Sperimentale, Macerata.

Mucciarelli, M., Albarello, D. and D'Amico, V. (2008) Comparison of probabilistic seismic hazard estimates in italy. *Bulletin of the Seismological Society of America*, **98**, 2652–2664.

Oliveti, I., Faenza, L., Antonucci, A., Locati, M., Rovida, A. and Michelini, A. (2023)

ShakeMap Atlas of historical earthquakes in Italy [Data set]. *Istituto Nazionale di Geofisica e Vulcanologia (INGV)*. URL: https://doi.org/10.13127/shakemaps/historical.

Oliveti, I., Faenza, L. and Michelini, A. (2022a) Inge: Intensity-ground motion dataset for italy. *Annals of Geophysics*, **65**, DM102.

— (2022b) New reversible relationships between ground motion parameters and macroseismic intensity for italy and their application in shakemap. *Geophysical Journal International*, **231**, 1117–1137. URL: https://doi.org/10.1093/gji/ggac245.

Oros, E., Placinta, A. O., Popa, M., Rogozea, M. and Paulescu, D. (2019) Attenuation of macroseismic intensity for crustal romanian earthquakes: Calibrating the bakun-wentworth's method. In *IOP Conference Series: Earth and Environmental Science*, vol. 362, 012026. IOP Publishing.

Pasolini, C., Albarello, D., Gasperini, P., D'Amico, V. and Lolli, B. (2008a) The attenuation of seismic intensity in italy, part ii: Modeling and validation. *Bulletin of the Seismological Society of America*, **98**, 692–708.

Pasolini, C., Gasperini, P., Albarello, D., Lolli, B. and D'Amico, V. (2008b) The attenuation of seismic intensity in italy, part i: Theoretical and empirical backgrounds. *Bulletin of the Seismological Society of America*, **98**, 682–691.

Provost, L. and Scotti, O. (2020) Quake-md: Open-source code to quantify uncertainties in magnitude–depth estimates of earthquakes from macroseismic intensities. *Seismological Research Letters*, **91**, 2520–2530.

Rovida, A. and Antonucci, A. (2021) EPICA - European PreInstrumental Earthquake CAtalogue, version 1.1 [Data set]. URL: https://doi.org/10.13127/EPICA.1.1.

Rovida, A., Antonucci, A. and Locati, M. (2022a) The european preinstrumental earthquake

636 catalogue EPICA, the 1000–1899 catalogue for the european seismic hazard model 2020.
637 *Earth System Science Data*, **14**, 5213–5231.

638 Rovida, A. and Locati, M. (2015) Archive of historical earthquake data for the european-
639 mediterranean area. In *Perspectives on European Earthquake Engineering and Seismology*,
640 359–369. Springer, Cham.

641 Rovida, A., Locati, M., Antonucci, A. and Camassi, R. (2017) Italian Archive of Historical
642 Earthquake Data (ASMI) [Data set]. URL: `https://doi.org/10.13127/asmi`.

643 Rovida, A., Locati, M., Camassi, R., Lolli, B. and Gasperini, P. (2020) The italian earthquake
644 catalogue CPTI15. *Bulletin of Earthquake Engineering*, **18**, 2953–2984.

645 Rovida, A., Locati, M., Camassi, R., Lolli, B., Gasperini, P. and Antonucci, A. (2022b)
646 Catalogo parametrico dei terremoti italiani (CPTI15), versione 4.0 [Data set]. URL:
647 `https://emidius.mi.ingv.it/CPTI15-DBMI15/`.

648 Russo, E., Felicetta, C., D'Amico, M. C., Sgobba, S., Lanzano, G., Mascandola, C., Pacor,
649 F. and Luzi, L. (2022) ITalian ACcelerometric Archive (ITACA), version 3.2 [Data set].
650 URL: `https://doi.org/10.13127/itaca.3.2`.

651 Schwarz, J., Beinersdorf, S., Kaufmann, S. and Langhammer, T. (2008) Damage scenarios
652 for central europe—reinterpretation of historical earthquakes.

653 Sieberg, A. (1923) *Geologische, physikalische und angewandte Erdbebenkunde*. G. Fischer,
654 Jena.

655 Sørensen, M., Stromeyer, D. and Grünthal, G. (2009) Attenuation of macroseismic intensity:
656 A new relation for the marmara sea region, northwest turkey. *Bulletin of the Seismological*
657 *Society of America*, **99**, 538–553.

658 Stirling, M. and Petersen, M. (2006) Comparison of the historical record of earthquake hazard

with seismic-hazard models for new zealand and the continental united states. *Bulletin of the Seismological Society of America*, **96**, 1978–1994.

Stromeyer, D. and Grünthal, G. (2009) Attenuation relationship of macroseismic intensities in central europe. *Bulletin of the Seismological Society of America*, **99**, 554–565.

Stucchi, M., Albini, P., Mirto, C. and Rebez, A. (2004) Assessing the completeness of italian historical earthquake data. *Annals of Geophysics*, **47**, 659–673. URL: `https://doi.org/10.4401/ag-3330`.

Teramo, A., Termini, D., Stillitani, E. and Bottari, A. (1996) The determination of the epicentre by a vectorial modelling of macroseismic intensity distribution. *Natural Hazards*, **13**, 101–117.

Tertulliani, A., Rossi, A., Cucci, L. and Vecchi, M. (2009) L'aquila (central italy) earthquakes: The predecessors of the april 6, 2009 event. *Seismological Research Letters*, **80**, 1008–1013.

Tomczak, M. (1998) Spatial interpolation and its uncertainty using automated anisotropic inverse distance weighting (idw)-cross-validation/jackknife approach. *Journal of Geographic Information and Decision Analysis*, **2**, 18–30.

Visini, F., Meletti, C., Rovida, A., D'Amico, V., Pace, B. and Pondrelli, S. (2022) An updated area-source seismogenic model (ma4) for seismic hazard of italy. *Natural Hazards and Earth System Sciences*, **22**, 2807–2827.

Wald, D. J., Quitoriano, V., Heaton, T. H., Kanamori, H., Scrivner, C. W. and Worden, C. B. (1999) Trinet "shakemaps": Rapid generation of peak ground motion and intensity maps for earthquakes in southern california. *Earthquake Spectra*, **15**, 537–555.

Worden, C., Thompson, E., Hearne, M. and Wald, D. (2017) Shakemap v4 manual: Technical manual, user's guide, and software guide. *U S. Geol. Surv.*

— (2020) Shakemap manual online: technical manual, user's guide, and software guide. *U. S. Geological Survey*. URL: `http://usgs.github.io/shakemap/`.

Worden, C., Wald, D., Allen, T., Lin, K., Garcia, D. and Cua, G. (2010) A revised ground-motion and intensity interpolation scheme for shakemap. *Bulletin of the Seismological Society of America*, **100**, 3083–3096.

Worden, C. B., Thompson, E. M., Baker, J. W., Bradley, B. A., Luco, N. and Wald, D. J. (2018) Spatial and spectral interpolation of ground-motion intensity measure observations. *Bulletin of the Seismological Society of America*, **108**, 866–875.

Zanini, M. A., Hofer, L. and Faleschini, F. (2019) Reversible ground motion-to-intensity conversion equations based on the EMS-98 scale. *Engineering Structures*, **180**, 310–320.

Full physical mailing address for each author:

- Ilaria Oliveti: Istituto Nazionale di Geofisica e Vulcanologia, Sezione ONT, via di Vigna Murata 605, 00143, Rome, Italy.
- Licia Faenza: Istituto Nazionale di Geofisica e Vulcanologia, Sezione di Bologna, viale Berti Pichat, 6/2, 40127, Bologna, Italy.
- Andrea Antonucci: Istituto Nazionale di Geofisica e Vulcanologia, Sezione di Milano, via Alfonso Corti 12, 20133, Milan, Italy.
- Mario Locati: Istituto Nazionale di Geofisica e Vulcanologia, Sezione di Milano, via Alfonso Corti 12, 20133, Milan, Italy.
- Andrea Rovida: Istituto Nazionale di Geofisica e Vulcanologia, Sezione di Milano, via Alfonso Corti 12, 20133, Milan, Italy.
- Alberto Michelini: Istituto Nazionale di Geofisica e Vulcanologia, Sezione ONT, via di Vigna Murata 605, 00143, Rome, Italy.

List of Figures

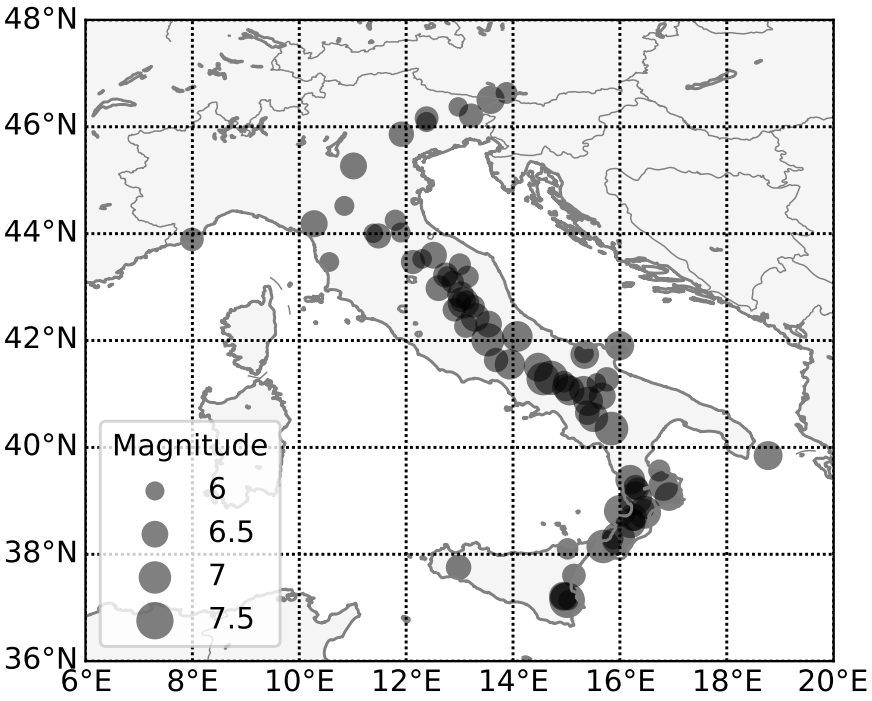

Figure 1: Spatial distribution of the selected seismic events (grey circles). Circle sizes are plotted relative to their magnitude value.

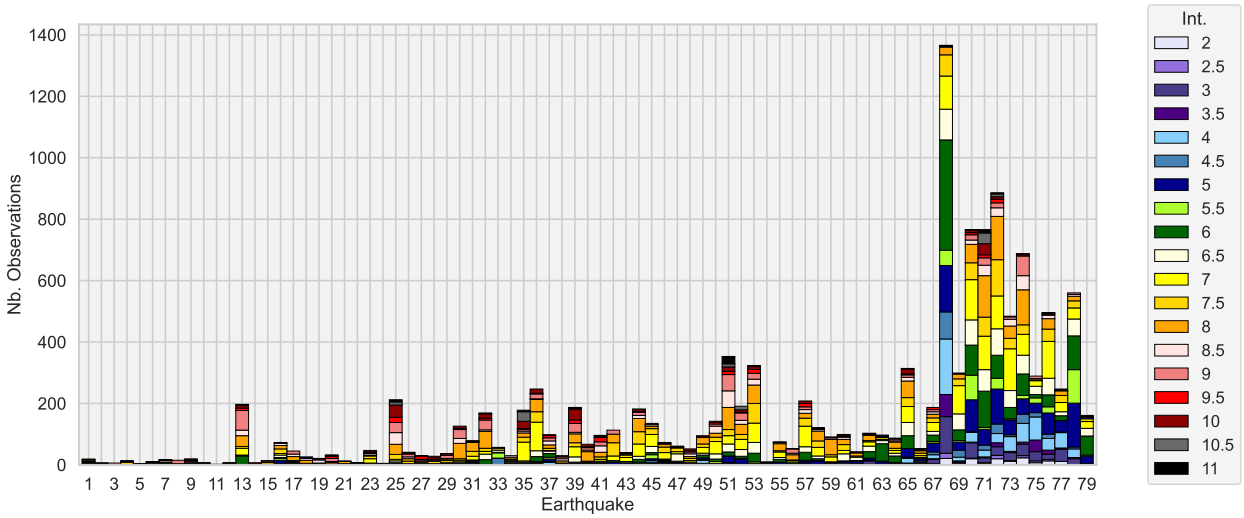

.

Figure 2: Number of MDPs extracted from DBMI15 per earthquake for different macroseismic intensities values. The dataset includes 79 earthquakes sorted in chronological order (from 1117 to 1968) following the numbering provided in Table 1

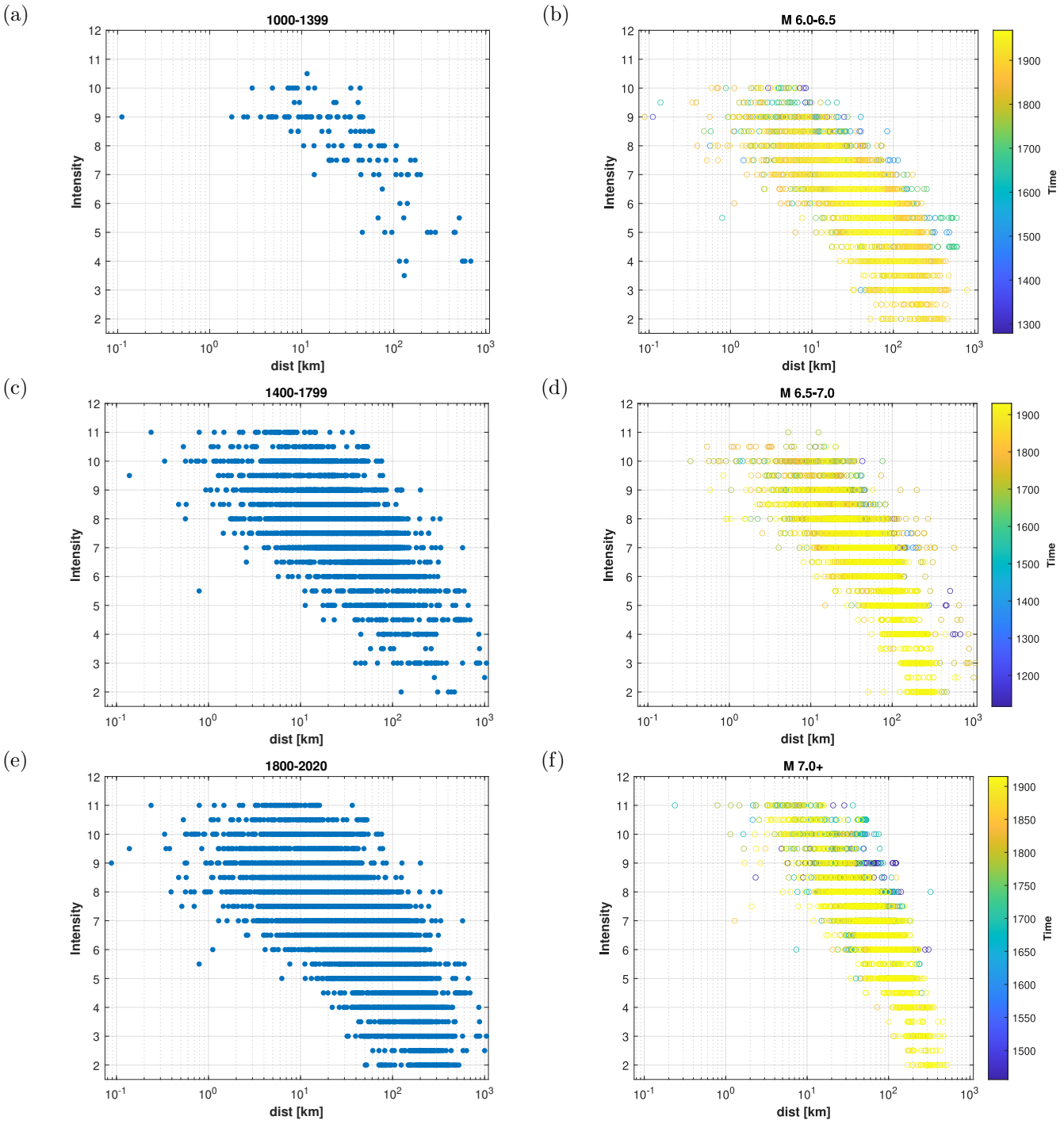

Figure 3: Earthquake distance coverage of the intensity dataset grouped by year (a, c, e) and magnitude ranges (b, d, f). The magnitude ranges are 6-6.5, 6.5-7.0 and 7-7.5, whereas the time slots are 1000-1399, 1400-1799 and 1800-2020. In the (b, d, f) panels the temporal color scale reflects the MDPs distribution of the (a, c, e) panels. Overall, the figure reveals that no significant bias affects the dataset.

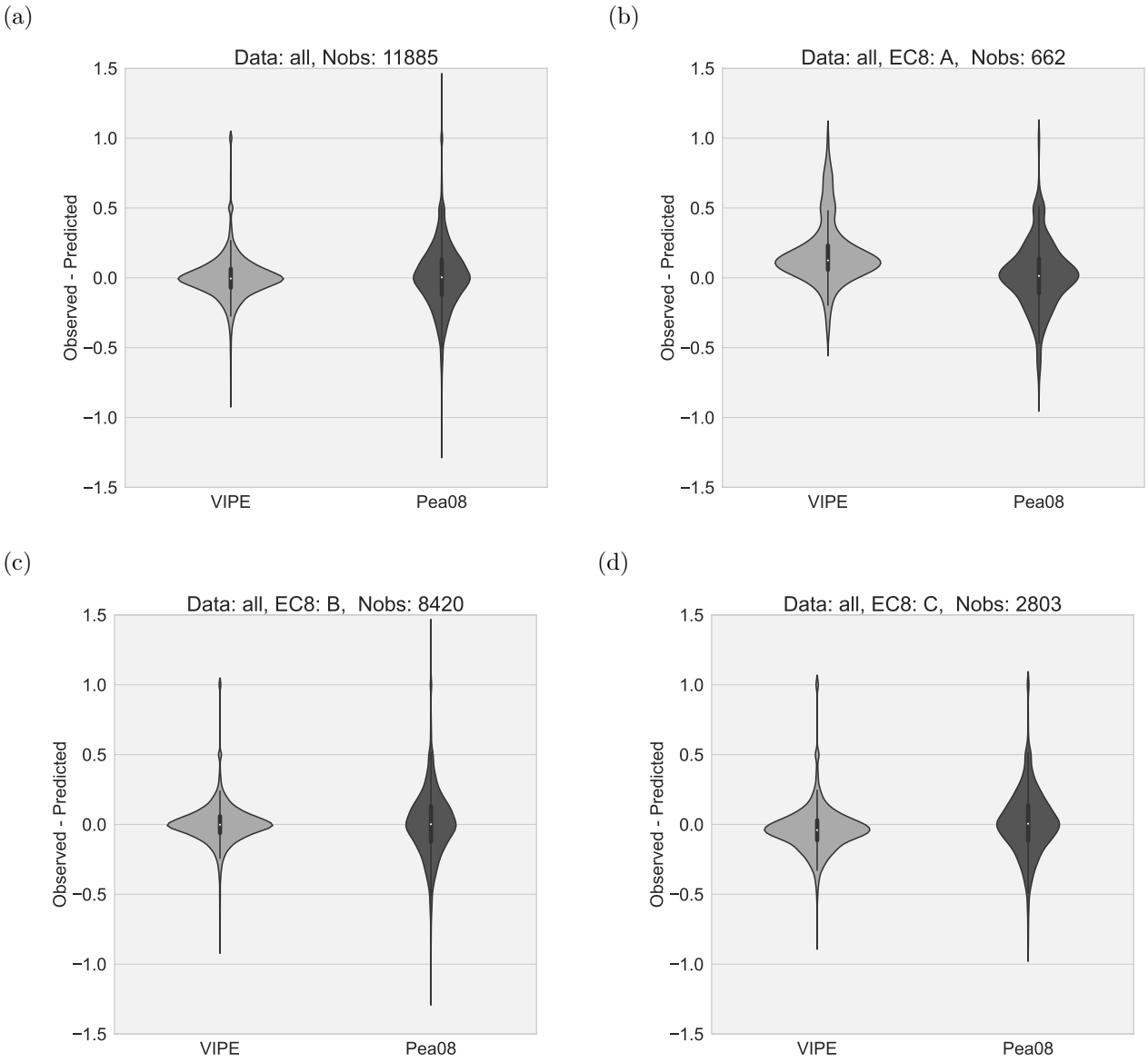

Figure 4: Violin plot diagram of the differences between observed and ShakeMap predicted intensity values for the entire validation dataset (79 earthquakes) and for the EC8 A-C classes disaggregated subsets, using the VIPE and Pea08 configurations: (a) All data, (b) EC8 class A data, (c) EC8 class B data, and (d) EC8 class C data. [Violin plots are a method of plotting numeric data through their median (the tiny white dot on the violin plot), interquartile range (the black bar in the center of violin) and the lower/upper adjacent values (the black lines stretched from the bar) — defined as first quartile ($-1.5\ IQR$) and third quartile ($+1.5IQR$), respectively].

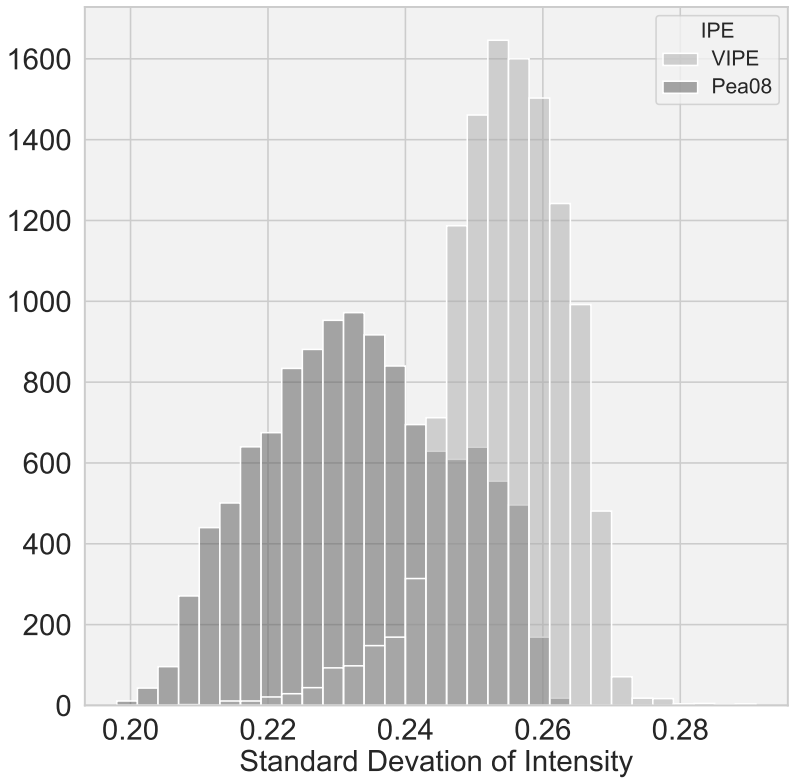

Figure 5: Histograms of the standard deviation distribution of the predicted intensity values at the 11885 macroseismic data points for the VIPE (light grey) and Pea08 (grey) configurations. The overall higher values of the VIPE distribution reflects the larger uncertainty in the predictions due to the additional uncertainty of the GMICEs.

(a) (b)

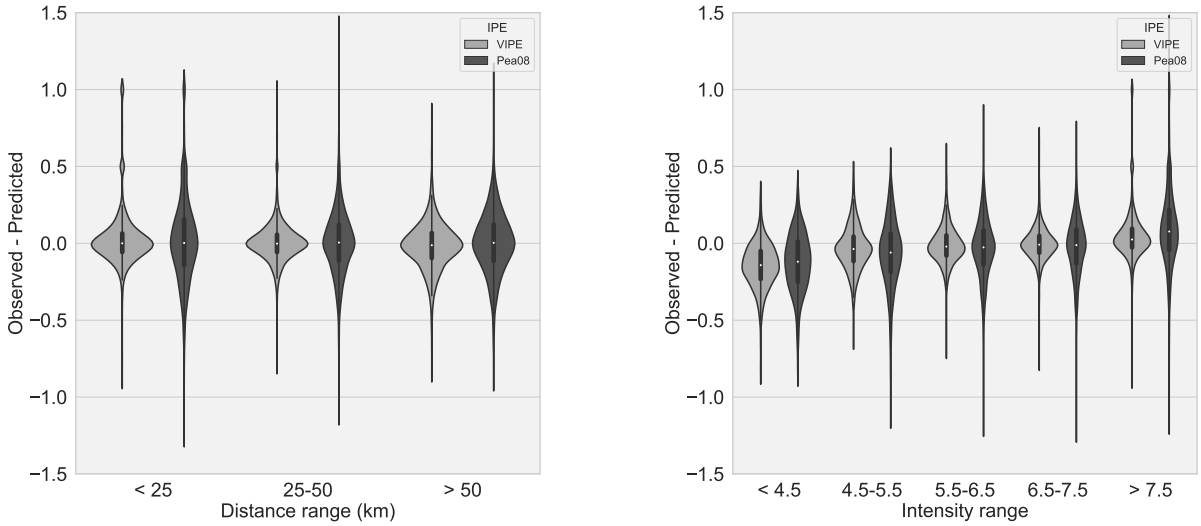

Figure 6: Violin plot diagram of the differences between observed and ShakeMap predicted intensity values for the entire validation dataset (79 earthquakes) resulting from the leave-one-out cross-validation test, using the VIPE and Pea08 configurations. The residuals are classified into (a) earthquake distance and (b) intensity categories.

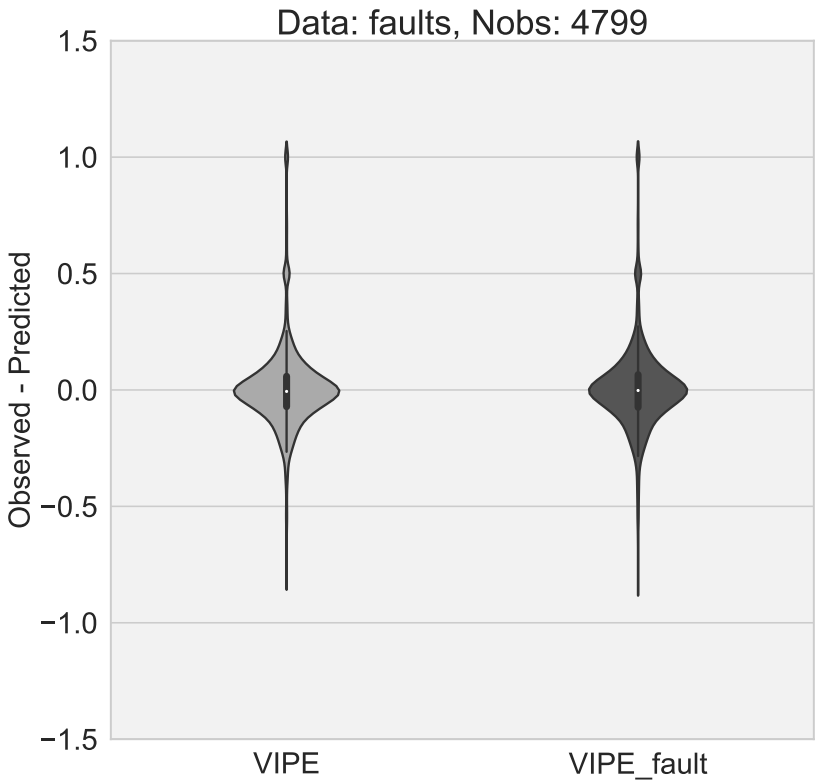

Figure 7: Violin plot diagram of the differences between observed and ShakeMap predicted intensity values for a subset of the validation dataset (16 of 79 earthquakes) resulting from the leave-one-out cross-validation test, using the VIPE configuration with and without the fault geometry. The faults and the focal mechanism parameters are provided by the DISS database (see Data and Resources; DISS Working Group, 2021).

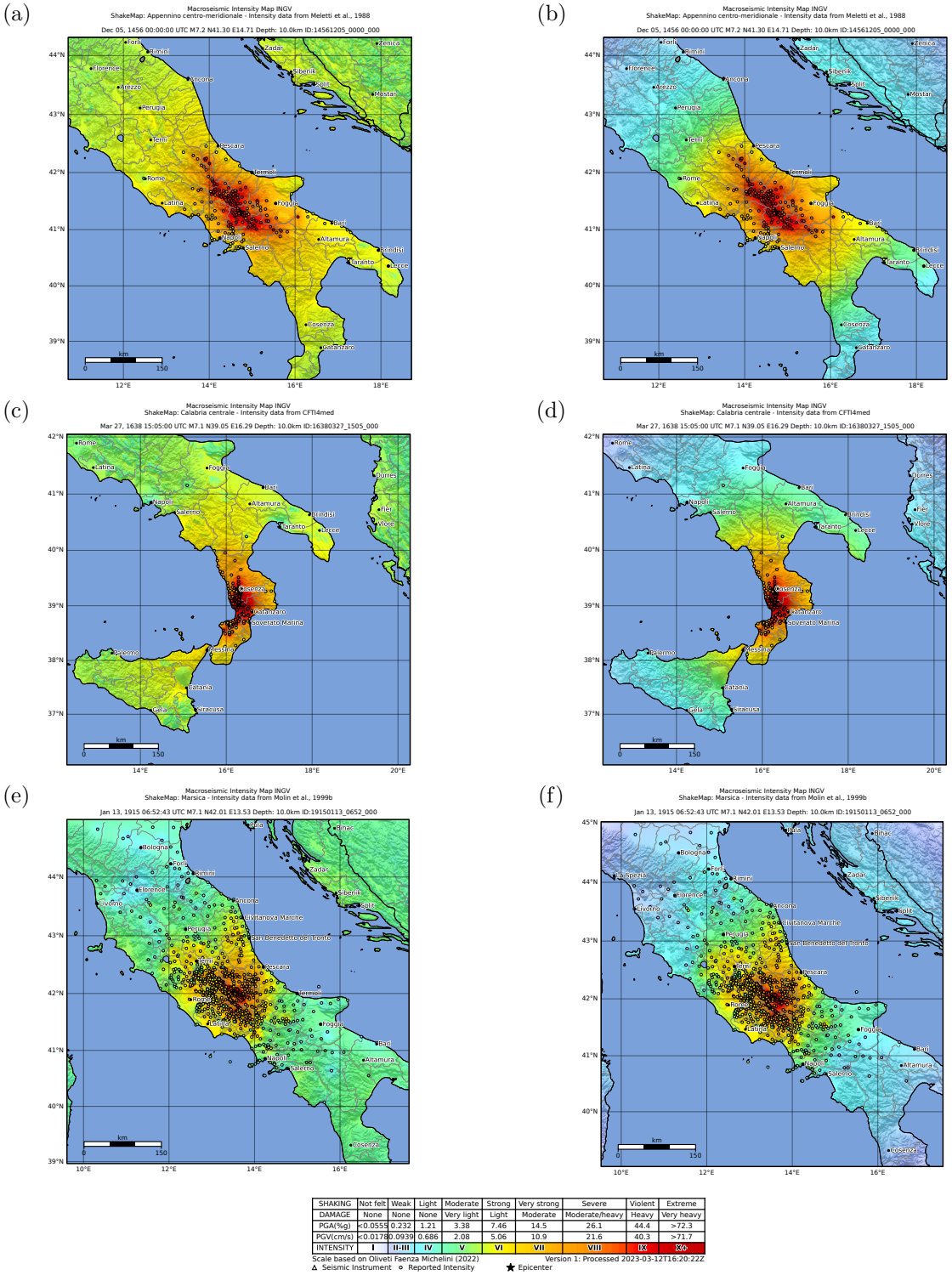

Figure 8: Intensity maps for the 5 December 1456 M 7.2, 27 March 1638 M 7.1, and 13 January 1915 M 7.1 earthquakes. The maps have been created using the v.4 of the U.S. Geological Survey (USGS)-ShakeMap software with the VIPE (a,c,e) and Pea08 (b,d,f) configurations.

Table 1: **List of the selected seismic events: event number and ID, time, epicenter, magnitude, number of macroseismic data, name of the epicentral area and the reference macroseismic study for each event are indicated.**

No.	Event-ID	Origin Time	Lat	Lon	Mag	MPDs	Epicentral Area	Reference
1	11170103_1515_000	1117-01-03T15:15:00Z	45.267	11.015	6.5	19	Veronese	Guidoboni et al. (2007)
2	11690204_0700_000	1169-02-04T07:00:00Z	37.215	14.949	6.5	7	Sicilia sud-orientale	Guidoboni et al. (2007)
3	11840524_0000_000	1184-05-24T00:00:00Z	39.395	16.193	6.8	6	Valle del Crati	Guidoboni et al. (2007)
4	12790430 1800_000	1279-04-30T18:00:00Z	43.093	12.872	6.2	13	Appennino umbro-marchigiano	Monachesi (1987)
5	12981201_0000_000	1298-12-01T00:00:00Z	42.575	12.902	6.3	4	Monti Reatini	Guidoboni et al. (2007)
6	13281201_0000_000	1328-12-01T00:00:00Z	42.857	13.018	6.5	11	Valnerina	Monachesi (1987)
7	13480125 1530_000	1348-01-25T00:00:00Z	46.504	13.581	6.6	17	Alpi Giulie	Caracciolo et al. (2015)
8	13490909_0000_000	1349-09-09T00:00:00Z	42.270	13.118	6.3	15	Appennino laziale-abruzzese	Guidoboni et al. (2007)
9	13490909 0815_001	1349-09-09T00:00:00Z	41.554	13.942	6.8	19	Lazio-Molise	Galli and Naso (2009)
10	13521225_0000_000	1352-12-25T00:00:00Z	43.469	12.127	6.3	7	Alta Valtiberina	Castelli et al. (1996)
11	13610717 1715_000	1361-07-17T17:15:00Z	41.205	15.561	6.0	2	Subappennino dauno	Guidoboni et al. (2007)
12	13891018_0000_000	1389-10-18T00:00:00Z	43.527	12.299	6.0	7	Alta Valtiberina	Castelli et al. (1996)
13	14561205_0000_000	1456-12-05T00:00:00Z	41.302	14.711	7.2	197	Appennino centro-meridionale	Meletti et al. (1988)
14	14611127 2105_000	1461-11-27T00:00:00Z	42.308	13.543	6.5	7	Aquilano	Tertulliani et al. (2009)
15	15010605 1000_000	1501-06-05T10:00:00Z	44.519	10.844	6.1	14	Modenese	Guidoboni et al. (2007)
16	15110326 1440_000	1511-03-26T15:30:00Z	46.209	13.216	6.3	73	Friuli-Slovenia	Camassi et al. (2011)
17	15420613 0215_000	1542-06-13T02:15:00Z	44.006	11.385	6.0	45	Mugello	Guidoboni et al. (2007)
18	15421210 1515_000	1542-12-10T15:15:00Z	37.215	14.944	6.7	26	Sicilia sud-orientale	Guidoboni et al. (2007)
19	15610731 1945_000	1561-07-31T19:45:00Z	40.650	15.389	6.3	21	Vallo di Diano	Castelli et al. (2008)
20	15610819 1550_000	1561-08-19T15:50:00Z	40.563	15.505	6.7	32	Vallo di Diano	Castelli et al. (2008)
21	15991106 0125_000	1599-11-06T01:25:00Z	42.724	13.021	6.1	13	Valnerina	Guidoboni et al. (2007)
22	16260404 1245_000	1626-04-04T12:45:00Z	38.851	16.456	6.1	7	Calabria centrale	Guidoboni et al. (2007)
23	16270730 1050_000	1627-07-30T10:50:00Z	41.737	15.342	6.7	47	Capitanata	Guidoboni et al. (2007)

24	16270807 1640_000	1627-08-07T16:40:00Z	41.758	15.328	6.0	5	Capitanata	Guidoboni et al. (2007)
25	16380327 1505_000	1638-03-27T15:05:00Z	39.048	16.289	7.1	212	Calabria centrale	Guidoboni et al. (2007)
26	16380608 0945_000	1638-06-08T09:45:00Z	39.279	16.812	6.8	41	Crotonese	Guidoboni et al. (2007)
27	16391007_0000_000	1639-10-07T00:00:00Z	42.639	13.261	6.2	30	Monti della Laga	Castelli (2003)
28	16460531_0000_000	1646-05-31T00:00:00Z	41.905	15.993	6.7	28	Gargano	Camassi et al. (2008)
29	16540724 0025_000	1654-07-24T00:00:00Z	41.635	13.683	6.3	37	Sorano	Guidoboni et al. (2007)
30	16591105 2215_000	1659-11-05T22:15:00Z	38.694	16.249	6.6	126	Calabria centrale	Guidoboni et al. (2007)
31	16610322 1250_000	1661-03-22T12:50:00Z	44.021	11.898	6.1	78	Appennino forlivese	Guidoboni et al. (2007)
32	16880605 1530_000	1688-06-05T15:30:00Z	41.283	14.561	7.1	169	Sannio	Guidoboni et al. (2007)
33	16901204 1400_000	1690-12-04T14:00:00Z	46.633	13.880	6.2	57	Carinthia, Villach	Guidoboni et al. (2007)
34	16930109 2100_000	1693-01-09T21:00:00Z	37.141	15.035	6.1	30	Sicilia sud-orientale	Guidoboni et al. (2007)
35	16930111 1330_000	1693-01-11T13:30:00Z	37.140	15.013	7.3	178	Sicilia sud-orientale	Guidoboni et al. (2007)
36	16940908 1140_000	1694-09-08T11:40:00Z	40.862	15.406	6.7	247	Irpinia-Basilicata	Guidoboni et al. (2007)
37	16950225 0530_000	1695-02-25T05:30:00Z	45.861	11.910	6.4	98	Asolano	Camassi et al. (2012)
38	17020314 0500_000	1702-03-14T05:00:00Z	41.120	14.989	6.6	30	Sannio-Irpinia	Guidoboni et al. (2007)
39	17030114 1800_000	1703-01-14T18:00:00Z	42.708	13.071	6.9	187	Valnerina	Guidoboni et al. (2007)
40	17030202 1105_000	1703-02-02T11:05:00Z	42.434	13.292	6.7	67	Aquilano	Guidoboni et al. (2007)
41	17061103 1300_000	1706-11-03T13:00:00Z	42.076	14.080	6.8	96	Maiella	Guidoboni et al. (2007)
42	17300512 0500_000	1730-05-12T05:00:00Z	42.753	13.120	6.0	113	Valnerina	Guidoboni et al. (2007)
43	17310320 0300_000	1731-03-20T03:00:00Z	41.274	15.757	6.3	40	Tavoliere delle Puglie	Guidoboni et al. (2007)
44	17321129 0740_000	1732-11-29T07:40:00Z	41.064	15.059	6.8	182	Irpinia	Guidoboni et al. (2007)
45	17410424 0900_000	1741-04-24T09:20:00Z	43.425	13.005	6.2	135	Fabrianese	Monachesi (1987)
46	17430220 1630_000	1743-02-20T00:00:00Z	39.847	18.774	6.7	72	Ionio settentrionale	Galli and Naso (2008)
47	17470417_0000_000	1747-04-17T00:00:00Z	43.204	12.769	6.1	61	Appennino umbro-marchigiano	Castelli (2003)
48	17510727 0100_000	1751-07-27T01:00:00Z	43.225	12.739	6.4	52	Appennino umbro-marchigiano	Guidoboni et al. (2007)
49	17810404 2120_000	1781-04-04T21:20:00Z	44.251	11.798	6.1	95	Faentino	Guidoboni et al. (2007)
50	17810603_0000_000	1781-06-03T00:00:00Z	43.596	12.512	6.5	142	Cagliese	Monachesi (1987)

51	17830205 1200_000	1783-02-05T12:00:00Z	38.297	15.970	7.1	353	Calabria meridionale	Guidoboni et al. (2007)
52	17830207 1310_000	1783-02-07T13:10:00Z	38.580	16.201	6.7	191	Calabria centrale	Guidoboni et al. (2007)
53	17830328 1855_000	1783-03-28T18:55:00Z	38.785	16.464	7.0	323	Calabria centrale	Guidoboni et al. (2007)
54	17860310 1410_000	1786-03-10T14:10:00Z	38.102	15.021	6.1	10	Golfo di Patti	Guidoboni et al. (2007)
55	17911013 0120_000	1791-10-13T01:20:00Z	38.636	16.268	6.1	75	Calabria centrale	Guidoboni et al. (2007)
56	17990728 2205_000	1799-07-28T22:05:00Z	43.193	13.151	6.2	53	Appennino marchigiano	Guidoboni et al. (2007)
57	18050726 2100_000	1805-07-26T21:00:00Z	41.500	14.474	6.7	208	Molise	Guidoboni et al. (2007)
58	18180220 1815_000	1818-02-20T18:15:00Z	37.603	15.140	6.3	121	Catanese	Guidoboni et al. (2007)
59	18320113 1300_000	1832-01-13T13:00:00Z	42.980	12.605	6.4	91	Valle Umbra	Guidoboni et al. (2007)
60	18320308 1830_000	1832-03-08T18:30:00Z	39.079	16.919	6.7	99	Crotonese	Guidoboni et al. (2007)
61	18360425 0020_000	1836-04-25T00:00:00Z	39.567	16.737	6.2	42	Calabria settentrionale	Guidoboni et al. (2007)
62	18460814 1200_000	1846-08-14T12:00:00Z	43.470	10.562	6.0	103	Colline Pisane	Guidoboni et al. (2007)
63	18510814 1320_000	1851-08-14T13:20:00Z	40.960	15.669	6.5	97	Vulture	Guidoboni et al. (2007)
64	18540212 1750_000	1854-02-12T17:50:00Z	39.256	16.295	6.3	87	Cosentino	Guidoboni et al. (2007)
65	18571216 2115_001	1857-12-16T21:15:00Z	40.352	15.842	7.1	314	Basilicata	Guidoboni et al. (2007)
66	18701004 1655_000	1870-10-04T16:55:00Z	39.220	16.331	6.2	53	Cosentino	Guidoboni et al. (2007)
67	18730629 0358_000	1873-06-29T03:58:00Z	46.159	12.383	6.3	187	Alpago Cansiglio	Guidoboni et al. (2007)
68	18870223 0521_000	1887-02-23T05:21:50.00	43.89	7.992	6.3	1366	Liguria occidentale	Guidoboni et al. (2007)
69	18941116 1752_000	1894-11-16T17:52:00Z	38.288	15.870	6.1	299	Calabria meridionale	Guidoboni et al. (2007)
70	19050908 0143_000	1905-09-08T01:43:00Z	38.811	16.000	7.0	766	Calabria centrale	Galli and Molin (2007)
71	19081228 0420_000	1908-12-28T04:20:27.00	38.14	15.68	7.1	766	Stretto di Messine	Guidoboni et al. (2007)
72	19150113 0652_000	1915-01-13T06:52:43.00	42.01	13.53	7.0	886	Marsica	Molin et al. (1999)
73	19190629 1506_000	1919-06-29T15:06:13.00	43.95	11.48	6.3	484	Mugello	Guidoboni et al. (2007)
74	19200907 0555_000	1920-09-07T05:55:40.00	44.18	10.27	6.5	688	Garfagna	Guidoboni et al. (2007)
75	19280327 0832_000	1928-03-27T08:32:00Z	46.372	12.975	6.0	289	Carnia	Barbano et al. (1990)
76	19300723_0008_000	1930-07-23T00:00:00Z	41.068	15.318	6.7	496	Irpinia	Galli et al. (2002)
77	19361018 0310_000	1936-10-18T03:10:00Z	46.089	12.380	6.1	247	Alpago Cansiglio	Barbano et al. (1986)

78	19620821 1819_000	1962-08-21T18:19:00Z	41.230	14.953	6.2	560	Irpinia	Gizzi (2012)
79	19680115 0201_000	1968-01-15T02:01:9.00Z	37.756	12.981	6.4	161	Valle del Belice	Guidoboni et al. (2007)

Table 2: **Statistical results in terms of median, mean, standard deviation (sd), first (Q1) and third quartiles (Q3) of the residuals. The comparison between the two Shakemap configurations (i.e, using VIPE and Pea08) is shown for the entire dataset and for data grouped according to the EC8 site classes.**

Dataset	**median**		**mean**		**sd**		**Q1**		**Q3**	
	VIPE	**Pea08**	**VIPE**	**Pea08**	**VIPE**	**Pea08**	**VIPE**	**Pea08**	**VIPE**	**Pea08**
All data	-0.0048	0.0034	0.0024	0.0075	0.16	0.23	-0.07	-0.12	0.06	0.13
EC8 class A	0.13	0.01	0.17	0.02	0.22	0.24	0.06	-0.11	0.23	0.14
EC8 class B	-0.0018	0.0017	0.002	0.005	0.15	0.24	-0.06	-0.13	0.06	0.13
EC8 class C	-0.040	0.005	-0.035	0.013	0.17	0.23	-0.11	-0.12	0.03	0.14

Table 3: **List of the selected faults from DISS: strike, dip and rake for each source are indicated.**

Event-ID	**DISS-ID**	**Strike(deg)**	**Dip(deg)**	**Rake(deg)**
11170103_1515_000	ITIS140	248	40	90
16930111_1330_000	ITIS074	57	45	70
16950225_0530_000	ITIS102	240	35	80
17030202_1105_000	ITIS015	132	50	270
17321129_0740_000	ITIS006	275	64	237
17810404_2120_000	ITIS093	108	35	90
17810603_0000_000	ITIS047	134	30	270
17830205_0000_000	ITIS012	30	30	270
17830207_1310_000	ITIS011	30	30	270
18050726_2100_000	ITIS004	304	55	270
18320113_1300_000	ITIS061	330	30	270
19081228_0420_000	ITIS013	30	29	270

19150113_0652_000	ITIS002	135	60	270
19190629_1506_000	ITIS086	298	40	270
19200907_0555_000	ITIS050	305	40	270
19300723_0008_000	ITIS088	280	64	237